ARTICLE

OBC
www.rsc.org/obc

Determining the σ-donor ability of the cyclopropane C–C bond

Nathan L. Fifer and Jonathan M. White*

School of Chemistry, The University of Melbourne, 3010, Melbourne, Australia.
E-mail: whitejm@unimelb.edu.au

Received 2nd March 2005, Accepted 21st March 2005
First published as an Advance Article on the web 11th April 2005

The low temperature crystal structures of ester and ether derivatives of varying electron demand, derived from cyclopropylmethanol **8** and dicyclopropylmethanol **9**, have been determined. These structures show a very strong response of the C–OR bond distance to the electron demand of the OR substituent, demonstrating the strong σ-donor ability of the strained C–C bonds in the cyclopropane ring.

Introduction

Interactions between donor orbitals and acceptor orbitals within a molecular framework can have a profound effect on fundamental molecular properties, including geometry and reactivity.[1] The strength of these interactions is dependant on both the intrinsic donor and acceptor abilities of the orbitals involved and upon their relative spatial relationships. These interactions often give rise to unusual chemical and spectroscopic properties and, because of their dependence on stereochemistry, they are frequently referred to as stereoelectronic effects.[2] Hyperconjugation (or σ–π conjugation)[3] is a particularly important type of donor–acceptor interaction between a filled σ-bonding orbital ($\sigma_{C\text{-}X}$) and an electron deficient orbital such as a carbocation p-orbital (Fig. 1).

Fig. 1 Hyperconjugation between σ_{CX} and a carbocation p-orbital.

The ease at which a C–X σ-bond donates electrons by hyperconjugation is an important fundamental property referred to as the σ-donor ability. Information on the relative donor abilities of a range of C–X bonds has been obtained by various means including Hammett plots,[4] measurement of the CT bands in donor–acceptor complexes,[5] ^{19}F and ^{13}C NMR spectroscopy[6] and by *ab initio* calculations on suitable model systems.[7] An X-ray structural method for obtaining information on the σ-donor abilities of bonds is the *variable oxygen probe*:[8,9] Kirby and coworkers established that the C–O bond distance in the C–OR fragment increases with increasing electron demand of the OR substituent, reflecting an increasing contribution of the C^+ $^-$OR valence bond form to the ground state structure. If the electron demand of a substituent OR is quantified as the pK_a value for the parent acid (ROH), then a plot of C–OR bond distance *vs.* pK_a(ROH) is linear and the slope of the resulting plot is sensitive to the effects of electron donation into the C–OR σ* antibonding orbital. The presence of good donor orbitals vicinal and antiperiplanar to the C–O bond results in a strong response of the C–OR distance to the electron demand of OR. This reflects increased stabilisation of the cation part of the valence bond form C^+ $^-$OR. For example, plots of C–OR bond distance *vs.* pK_a(ROH) constructed for **1**,[8] **2**[10] and **3**[11] gave the following relationships:

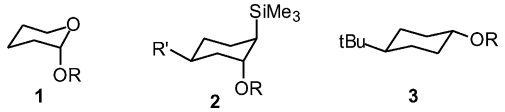

1 2 2 2

$$r_{C\text{-}O}/\text{Å} = 1.49\text{–}6.49 \times 10^{-3}\ \text{p}K_a(\text{ROH})\ R^2 = 0.985 \quad (1)$$

$$r_{C\text{-}O}/\text{Å} = 1.50\text{–}5.30 \times 10^{-3}\ \text{p}K_a(\text{ROH})\ R^2 = 0.986 \quad (2)$$

$$r_{C\text{-}O}/\text{Å} = 1.48\text{–}2.77 \times 10^{-3}\ \text{p}K_a(\text{ROH})\ R^2 = 0.976 \quad (3)$$

A strong response of C–OR bond distance to the electron demand of OR is demonstrated for **1**, which has oxygen lone pair (n_O) orbital antiperiplanar to the OR substituent (this is the basis of the well known anomeric effect).[12] A strong response is also observed for **2**, which has a C–Si bond antiperiplanar to the OR substituent (this is the basis of the silicon β-effect),[1,13] but a weaker response is obvious in **3**, having a $\sigma_{C\text{-}C}$ bonding orbital, which is a weaker donor orbital situated antiperiplanar to the OR bond.

Subsequently we became interested in applying this structural technique to molecules with carbon skeletons containing strained σ-bonds, particularly cyclopropyl-substituted systems. The effect of the strain in the three-membered ring increases the energy of the $\sigma_{C\text{-}C}$ orbital and hence increases its σ-donor ability.[14,15,16,17] Consistent with this, cyclopropyl substituents have been shown to facilitate the formation of carbocations on the adjacent carbon compared to their non-strained analogs.[18,19,20] For example, the relative rates of unimolecular solvolysis of the isopropyl- and cyclopropyl-substituted esters **4** and **5** are 1 : 503 000, indicating a high degree of hyperconjugative stabilisation of the intermediate cation **7** relative to **6**.

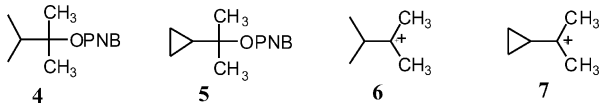

4 **5** **6** **7**

The model systems **8** and **9** were chosen for this study. Application of the variable oxygen probe to these cyclopropyl-substituted systems was hoped to not only give information on the donor ability of the strained C–C bonds, but might also reveal other interesting structural effects arising from interaction between the cyclopropyl $\sigma_{C\text{-}C}$ orbital and the $\sigma^*_{C\text{-}O}$ antibonding orbital.

Results and discussion

The alcohols **8** and **9** were readily prepared from commercially available starting materials and were converted to the crystalline ester and ether derivatives **8a–8f** and **9a–9d** using standard methods.

The derivatives of dicyclopropylmethanol **9** were found to be more difficult to handle than the monocyclopropyl derivatives and decomposed slowly in solution. Unfortunately the picrate derivative of **9** was too reactive to prepare and decomposed during the work up procedure.

DOI: 10.1039/b503124a

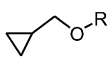

8; R = H
8a; R = 2,4,6-$(NO_2)_3C_6H_2$-
8b; R = 2,4-$(NO_2)_2C_6H_3CO$-
8c; R = 2,4-$(NO_2)_2C_6H_3S$-
8d; R = 3,5-$(NO_2)_2C_6H_3CO$-
8e; R = 4-$(NO_2)C_6H_4CO$-
8f; R = 4-NO_2-C_6H_4-

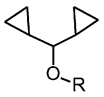

9; R = H
9a; R = 2,4-$(NO_2)_2C_6H_3CO$-
9b; R = 2,4-$(NO_2)_2C_6H_3S$-
9c; R = 3,5-$(NO_2)_2C_6H_3CO$-
9d; R = 4-$(NO_2)C_6H_4CO$-

The X-ray structures of **8a–8f** and **9a–9d** were determined at 130 K to minimise the unwanted effects of thermal motion. Unfortunately the 2,4-dinitrobenzoate derivative **8b** and the 3,5-dinitrobenzoate derivatives **9c** were disordered in the solid-state and the data could not be used in this study. Crystal data and structure refinement details are presented in Table 1.† Selected thermal ellipsoid plots (for **8a** and **9a**) are shown in Fig. 2 and Fig. 3 respectively and show the atom numbering scheme common to both sets of structures.

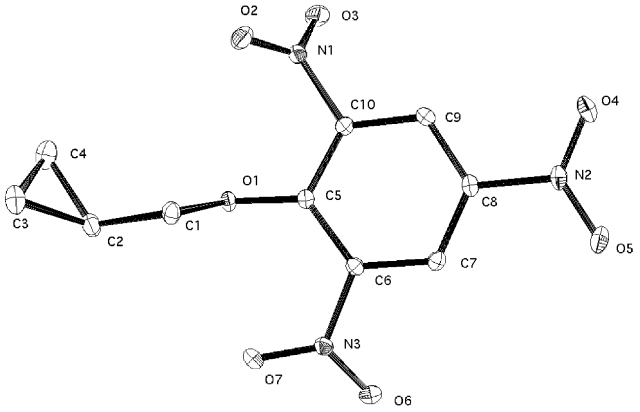

Fig. 2 Thermal ellipsoid plot of **8a**. Ellipsoids are at the 20% probability level.

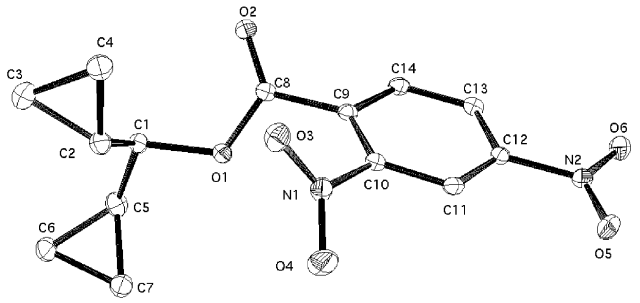

Fig. 3 Thermal ellipsoid plot of **9a**. Ellipsoids are at the 20% probability level.

For each of the monocyclopropyl esters **8a** and **8c–8f** the C2–C3 bond of the cyclopropyl ring is approximately *antiperiplanar* to the C1–O1 bond, while the C2–C4 bond is approximately *gauche* to the C1–O1. Similarly, in the dicyclopropyl substituted esters the C2–C3 and C5–C6 bonds are *antiperiplanar* to the C1–O1 bond while the C2–C4 and C5–C7 bonds are *gauche*.

Selected bond distances, angles and dihedral angles for the monocyclopropyl derivatives **8a** and **8c–8f** are presented in Table 2. Examination of this data reveals a clear relationship between the C1–O1 bond distance and the electron demand of the oxygen substituent (as estimated by the pK_a (ROH)), with the C1–O1 bond distance increasing with increasing electron demand of the oxygen substituent. Thus, the weakly electron demanding 4-nitrophenoxide derivative **8f** has a C1–O1 bond distance of 1.446(2) Å, whereas the picrate derivative **8a** has a C–OR distance of 1.479(2) Å which is significantly longer.

This data is presented graphically in Fig. 4 and gives rise to the following relationship between C1–O1 bond distance and the pK_a (ROH):

$$r_{C\text{–}O}/\text{Å} = 1.48\text{–}4.6 \times 10^{-3}\ \text{p}K_a(\text{ROH})\ R^2 = 0.94 \qquad (4)$$

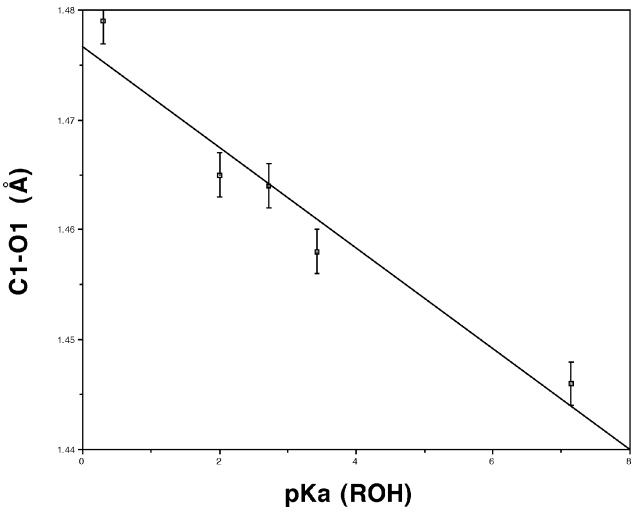

Fig. 4 r(C–O) *vs.* pK_a(ROH) relationship for the derivatives **8a** and **8c–8f**.

The slope of this plot for the cyclopropyl derivatives **8a** and **8c–8f** is -4.6×10^{-3}, which demonstrates a much stronger response of C–OR distance to the electron demand of the –OR substituent than was observed in simple, unsubstituted equatorial cyclohexyl-oxy derivatives (-2.77×10^{-3}) (eqn. 3). This is consistent with our expectation that the strained cyclopropyl $\sigma_{C\text{–}C}$ orbital should be a stronger σ-donor than the unstrained cyclohexane C–C bonds in **3**. Evidence that the strong response of the C1–O1 bond distance to the electron demand of the –OR substituent does indeed reflect σ-donation from a cyclopropane C–C bond is provided by examining the different C–C bond distances in the cyclopropane ring. The O1–C1–C2–C3 dihedral angle for these structures lie in the range −140–150°, which allows for close to optimum overlap between the C2–C3 'bent' σ-bonding orbital with the C1–O1 σ*-antibonding orbital (Fig. 5).

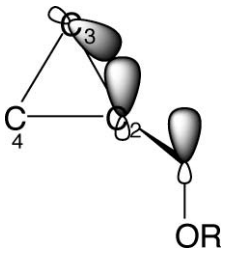

Fig. 5 σ_{CC}–σ^*_{CO} in cyclopropylmethanol derivatives.

By comparison the O1–C1–C2–C4 dihedral angles for **8a** and **8c–8f** lie in the range 70–90° and therefore overlap between the C2–C4 bond and the C1–O1 σ*-antibonding orbital would be much less effective. Consistent with this, the C2–C3 (donor) bond is longer than the C2–C4 bond in all cases and the difference between these two bonds (Δ) is more apparent for the strongly electron demanding substituents in **8a** and **8c–8f**.

The $\sigma_{C2\text{–}C3}$–$\sigma^*_{C1\text{–}O1}$ interaction is expected to impart some double bond character into the C1–C2, this bond distance does indeed decrease slightly from the weakly electron demanding 4-nitrophenoxide **8f** to the strongly demanding picrate **8a**. The dependence of the cyclopropyl C–C bond distances in **8a** and **8c–8f** on the C–C–C–O dihedral angle is reminiscent of previous studies on molecules containing cyclopropyl-substituted ketone fragments using the Cambridge Crystallographic Data Base.[21]

Table 1 Crystal data and structure refinement details for compounds **8a, 8c–8f** and **9a, 9b, 9d**

	8a	**8c**	**8d**	**8e**	**8f**	**9a**	**9b**	**9d**
Empirical formula	$C_{10}H_9N_3O_7$	$C_{10}H_{10}N_2OS$	$C_{11}H_{10}N_2O_6$	$C_{11}H_{11}NO_4$	$C_{10}H_{11}NO_3$	$C_{14}H_{14}N_2O_6$	$C_{13}H_{14}N_2O_5S$	$C_{14}H_{15}NO_4$
Formula weight	283.20	270.26	266.21	221.21	193.20	306.27	310.32	261.27
Temperature/K	130.0(1)	130.0(1)	130.0(1)	130.0(1)	130.0(1)	130.0(1)	130.0(1)	130.0(1)
Radiation	MoKα	MoKα	MoKα	MoKα	MoKα	MoKα	MoKα	MoKα
Wavelength/Å	0.71073	0.71073	0.71073	0.71073	0.71073	0.71073	0.71073	0.71073
Crystal system	Orthorhombic	Monoclinic	Orthorhombic	Monoclinic	Monoclinic	Monoclinic	Monoclinic	Monoclinic
Space group	$P2_12_12_1$	$P2_1/c$	$Pna2_1$	$P2_1/c$	$P2_1/c$	$P2_1/n$	$P2_1/c$	$P2_1/n$
Unit cell dimensions								
a	6.1596(6)	5.1517(14)	10.1620(8)	11.503(2)	11.1796(17)	14.0459(19)	10.3778(8)	6.9505(8)
b	7.9020(8)	11.726(3)	21.4665(17)	7.7574(16)	7.2234(11)	7.8502(11)	12.0317(10)	28.848(3)
c	24.235(2)	18.705(5)	5.4350(4)	12.737(3)	12.745(2)	14.279(2)	11.3503(9)	7.3706(8)
α								
β		94.289(5)		111.040(4)	115.033(3)	115.424(2)	104.395(2)	β = 116.961(2)
γ								
Volume/Å^3	1179.6(2)	1126.8(5)	1185.60(16)	1060.8(4)	932.5(2)	1422.0(3)	1372.73(19)	1317.2(2)
Z	4	4	4	4	4	4	4	4
D_c/Mg m^3	1.595	1.593	1.491	1.385	1.376	1.431	1.502	1.317
μ/mm^{-1}	0.138	0.303	0.124	0.107	0.103	0.114	0.260	0.097
F(000)	584	560	552	464	408	640	648	552
Crystal size	0.35 × 0.30 × 0.10	0.50 × 0.08 × 0.05	0.34 × 0.30 × 0.12	0.50 × 0.45 × 0.05	0.30 × 0.15 × 0.01	0.50 × 0.15 × 0.05	0.35 × 0.30 × 0.20	0.4 × 0.4 × 0.05
θ range/°	1.68 to 27.5	2.05 to 25.00	1.90 to 27.51	1.90 to 25.00	2.01 to 27.59	1.70 to 25.00	2.03 to 25.00	1.41 to 25.00
Index ranges	$-7 <= h <= 6$	$-6 <= h <= 5$	$-11 <= h <= 13$	$-13 <= h <= 12$	$-14 <= h <= 13$	$-16 <= h <= 16$	$-12 <= h <= 11$	$-6 <= h <= 8$
	$-10 <= k <= 7$	$-13 <= k <= 13$	$-27 <= k <= 21$	$-9 <= k <= 6$	$-9 <= k <= 8$	$-9 <= k <= 9$,	$-14 <= k <= 14$	$-34 <= k <= 27$
	$-31 <= l <= 30$	$-20 <= l <= 22$	$-6 <= l <= 7$	$-15 <= l <= 14$	$-16 <= l <= 16$	$-16 <= l <= 16$	$-13 <= l <= 12$	$-8 <= l <= 8$
Absorption method		Multiscan	Multiscan					
Max. min. transmission		1.0 and 0.74	1.0 and 0.9					
Refx collected	7329	5769	7145	4383	5551	9945	7185	6862
Independent	2651	1981	2625	1833	2115	2498	2422	2321
R(int)	0.0358	0.0887	0.0356	0.0785	0.0798	0.0849	0.0444	0.0737
Observed ($I > 2\sigma(I)$)	2383	1502	2532	1267	1392	2155	1999	1886
Data/restraints/param.	2651/0/181	1981/0/164	2625/1/173	1833/0/146	2115/0/127	2498/0/256	2422/0/190	2321/0/173
GOF on F^2	1.007	1.023	1.055	0.940	0.941	1.044	0.975	1.001
Final *R* indices [$I > 2\sigma(I)$]	$R1 = 0.0381$	$R1 = 0.0545$	$R1 = 0.0375$	$R1 = 0.0460$	$R1 = 0.0496$	$R1 = 0.0379$	$R1 = 0.0381$	$R1 = 0.0410$
	$wR2 = 0.0793$	$wR2 = 0.1061$	$wR2 = 0.0915$	$wR2 = 0.0923$	$wR2 = 0.1028$	$wR2 = 0.1012$	$wR2 = 0.0853$	$wR2 = 0.0964$
R indices (all data)	$R1 = 0.0433$	$R1 = 0.0746$	$R1 = 0.0390$	$R1 = 0.0702$	$R1 = 0.0783$	$R1 = 0.0426$	$R1 = 0.0480$	$R1 = 0.0512$
	$wR2 = 0.0814$	$wR2 = 0.1137$	$wR2 = 0.0924$	$wR2 = 0.0991$	$wR2 = 0.1123$	$R2 = 0.1037$	$wR2 = 0.0888$	$wR2 = 0.1006$
Weighting scheme[a]	$A = 0.0411$	$A = 0.0352$	$A = 0.0548$	$A = 0.0345$	$A = 0.0381$	$A = 0.0505$	$A = 0.0449$	$A = 0.0464$
	$B = 0.000$	$B = 0$	$B = 0.0122$	$B = 0$	$B = 0$	$B = 0.2699$	$B = 0$	$B = 0$
Extinction coefficient	0	0.0003(6)	0.0001(13)	0.0002(16)	0	0.0017(10)	0	0
Largest diff. peak and hole/eÅ^{-3}	0.22–0.20	0.267–0.360	0.252–0.210	0.213–0.160	0.231–0.217	0.28–0.17	0.311–0.244	0.23–0.20

[a] $w = 1/[\sigma^2(F_o^2) + (A*P)^2 + B*P]$; where $P = (F_o^2 + 2F_c^2)/3$.

Table 2 Selected bond distances (Å) and dihedral angles (°) for the derivatives of cyclopropylmethanol **8**

Compound	**8a**	**8c**	**8d**	**8e**	**8f**
pK_a (ROH)	0.3	2.0	2.8	3.4	7.2
O1–C1/Å	1.479(2)	1.465(3)	1.464(2)	1.458(2)	1.446(2)
C1–C2	1.478(3)	1.480(4)	1.491(2)	1.485(3)	1.489(2)
C2–C3	1.490(3)	1.501(4)	1.504(2)	1.498(3)	1.504(2)
C2–C4	1.470(3)	1.482(4)	1.494(2)	1.491(3)	1.495(2)
Δ^a/Å	0.02	0.019	0.010	0.007	0.009
C3–C4	1.487(3)	1.484(4)	1.492(3)	1.490(3)	1.492(2)
O1–C1–C2	107.49(14)	107.5(3)	108.5(2)	109.2(2)	108.5(1)
O1–C1–C2–C3	−151.4(2)	−141.9(3)	−149.6(2)	−157.7(2)	−143.4(1)
O1–C1–C2–C4	−81.8(2)	−72.4(4)	−81.1(2)	−88.6(2)	−74.7(2)

[a] Δ represents the difference between the C2–C3 and C2–C4 bond distances.

Table 3 Selected bond distances (Å) and dihedral angles (°) for the derivatives of dicyclopropylmethanol **9**

Compound	**9a**	**9b**	**9d**
O1–C1	1.492(2)	1.485(2)	1.476(2)
C1–C2	1.481(2)	1.494(2)	1.495(2)
C1–C5	1.503(2)	1.491(3)	1.499(2)
C2–C3	1.504(2)	1.498(2)	1.499(2)
C2–C4	1.488(2)	1.496(2)	1.503(2)
C5–C6	1.497(2)	1.506(2)	1.500(2)
C6–C7	1.497(2)	1.499(2)	1.497(3)
O1–C1–C2	106.9(1)	105.2(2)	110.8(1)
O1–C1–C5	105.5(1)	111.9(2)	105.1(1)
O1−C1−C2−C3	150.6(1)	148.3(2)	−168.1(1)
O1–C1–C2–C4	80.6(2)	77.9(2)	−98.4(2)
O1–C1–C5–C6	136.0(2)	−156.0(2)	140.3(2)
O1–C1–C5–C7	65.0(2)	−86.1(2)	70.9(2)

Selected bond distances, angles and dihedral angles for the dicyclocyclopropyl derivatives **9a**, **9b** and **9d** are presented in Table 3. This data also reveals a relationship between the C1–O1 bond distance and the electron demand of the oxygen substituent with the C1–O1 bond distance increasing with increasing electron demand of the oxygen substituent.

This smaller dataset is presented graphically in Fig. 6 and gives rise to the following relationship between C1–O1 bond distance and the pK_a (ROH):

$$r_{C\text{–}O}/\text{Å} = 1.50\text{–}7.7 \times 10^{-3}\ \text{p}K_a(\text{ROH})\ R^2 = 0.98 \qquad (5)$$

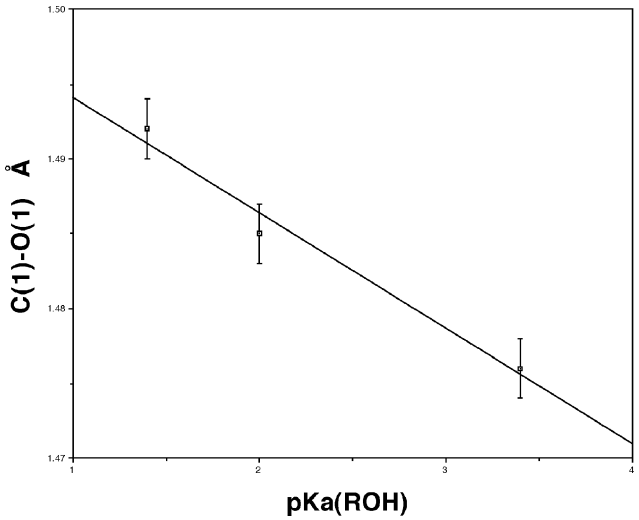

Fig. 6 r(C–O) *vs.* pK_a(ROH) relationship for the derivatives **9a**, **9b** and **9d**.

The pK_a (ROH) range spanned by the structures **9a**, **9b** and **9d** is small compared with the monocyclopropyl derivatives **8a** and **8c–8f**, however there is clearly a much stronger response of the C1–O1 bond distance to the electron demand of the OR substituent, consistent with the presence of the second strongly donating cyclopropyl substituent. In fact, the effects of the second ring are almost additive. The cyclopropane C–C bonds show much less variation than was the observed in the monocyclopropyl derivatives, presumable due to the structural effects of the σ_{CC}–σ^*_{CO} interaction being diluted over the two cyclopropyl rings.

Conclusion

Application of the variable oxygen probe to derivatives of cyclopropylmethanol **8** and dicyclopropylmethanol **9** demonstrates a very strong response of the C–OR bond distance to the electron demand of the OR substituent consistent with an enhanced σ-donor ability of strained C–C bonds compared with those in the unstrained cyclohexane ring. Consistent with this is the observation of systematic effects on the cyclopropane C–C bond distances with varying electron demand of the OR substituent.

Experimental

Synthesis

Anhydrous tetrahydrofuran and diethyl ether were distilled from sodium benzophenone ketyl and sodium metal under a nitrogen atmosphere. Anhydrous pyridine was distilled from calcium hydride and stored over 4 Å molecular sieves. Petroleum ether (petrol) refers to the fraction boiling at 40–60 °C. Benzoyl chlorides were prepared by stirring the benzoic acid derivative and oxalyl chloride (2 eq.) in CH_2Cl_2 with a catalytic amount of DMF at rt overnight. The crude benzoyl chloride derivative then underwent appropriate purification. Cyclopropylmethanol and dicyclopropylketone were purchased from the Aldrich Chemical Company and all other commercial reagents were used as received. Where necessary, all reactions of air and moisture sensitive compounds were performed in flame-dried glassware under a nitrogen atmosphere, which was purified by passage over activated 4 Å molecular sieves and BASF R3-11 copper catalyst. All melting points were determined on single crystals using a Reichert-Jung hot stage melting point apparatus and are uncorrected. All proton nuclear magnetic resonance (^{1}H NMR) and proton decoupled carbon nuclear magnetic resonance (^{13}C NMR) spectra were recorded in deuterochloroform solutions at ambient temperature with residual chloroform as the internal reference.

Dicyclopropylmethanol 9[22]. Dicyclopropyl ketone (5.0 g, 0.045 mol) in anhydrous ether (50 ml) was added dropwise to a solution of lithium aluminium hydride in ether (55 ml, 1.0 M, 0.055 mol) under N_2 at 0 °C then stirred for 1 h. The reaction was quenched with the sequential dropwise addition of water (2 ml), 10% NaOH (2 ml) then water (6 ml) to give fluffy white pellets. The solution was filtered, diluted with ether (50 ml), washed with water (2 × 100 ml) and the organic phase dried ($MgSO_4$).

Solvent was then removed under a reduced pressure to give a clear oil (4.5 g, 0.0401 mol, 89%). ^{1}H NMR 300 MHz δ 0.24 (m, 4H), 0.44 (m, 4H), 0.96 (m, 2H), 1.95 (bs, 1H), 2.38 (t, 1H); ^{13}C NMR δ ($CDCl_3$) 79.8, 16.8, 2.0.

Cyclopropylmethyl picrate 8a. A solution of cyclopropylmethanol **8** (0.07 g, 97 mmol) in CH_2Cl_2 (20 ml) and triethylamine (0.8 ml) was treated with 2,4,6-trinitrofluorobenzene (0.29 g, 0.76 mmol). After stirring for 3 h the solution was washed with water (3 × 20 ml), HCl (0.1 M, 2 × 20 ml) and then 5% aqueous $NaHCO_3$ (1 × 20 ml), dried ($MgSO_4$) and evaporated under a reduced pressure to afford a yellow solid. Crystallised from methanol gave **8a** (190 mg) as yellow slabs (mp 143–145 °C). ^{1}H NMR δ ($CDCl_3$) 9.15 (s, 2H), 4.12 (d, J = 7.3, 2H), 1.3 (m, 1H), 0.66 (m, 2H), 0.34 (m, 2H); ^{13}C NMR δ ($CDCl_3$) 149.7, 145.1, 140.2, 123.1, 84.4, 10.5, 3.7.

Cyclopropylmethyl *p*-nitrophenoxide 8f. Cyclopropyl methanol **8** (107 mg, 1.48 × 10^{-3} mol) was added to a slurry of NaH (90 mg, 3.8 × 10^{-3} mol) in anhydrous THF (50 ml) at 0 °C. The mixture was stirred for 1 h under N_2 then treated with *p*-fluoronitrobenzene (0.239 g, 1.69 × 10^{-3} mol) and stirred overnight. The mixture was diluted with water (50 ml), extracted into ether (3 × 50 ml) and the combined ether extracts washed with water (3 × 100 ml). The organic phase was dried ($MgSO_4$), filtered and the solvent removed under a reduced pressure to yield the ether **8f** as an oil which slowly crystallised at low temperature (mp 9–10 °C) (150 mg, 57%). ^{1}H NMR δ ($CDCl_3$) 0.35 (m, 2H), 0.61 (m, 2H), 0.80 (m, 1H), 3.85 (d, J = 6.8 Hz, 2H), 6.9 (d, J = 7.6 Hz, 2H), 8.1 (d, J = 7.6 Hz, 2H); ^{13}C NMR δ ($CDCl_3$) 163.9, 141.1, 125.6, 114.3, 73.3, 9.8, 3.0.

General synthesis of ester derivatives. Cyclopropylmethanol **8** (103 mg, 1.43 × 10^{-3} mol) and *p*-nitrobenzoyl chloride (333 mg, 1.79 × 10^{-3} mol) were stirred together in pyridine (1 ml) under N_2 for four hours. Water (1–2 drops) was added to quench the reaction, the product was extracted into ether (3 × 50 ml) and the combined organic extracts washed with sat. $CuSO_4$ solution (2 × 50 ml), water (50 ml) and $NaHCO_3$ (50 ml). The organic phase was dried ($MgSO_4$) and solvent removed under a reduced pressure to yield cyclopropylmethyl *p*-nitrobenzoate **8e** (250 mg, 1.1 × 10^{-3}, 79%). The product was crystallised from hot ether (mp 52–55 °C, lit[23] 56–57 °C). ^{1}H NMR δ ($CDCl_3$) 0.39 (m, 2H,), 0.65 (m, 2H), 1.22 (m, 1H,), 4.20 (d, 2H, J = 7.3 Hz), 8.24 (d, 2H, J = 8.7 Hz), 8.29 (d, 2H, J = 8.7 Hz); ^{13}C NMR δ ($CDCl_3$) 164.7, 150.4, 135.8, 130.6, 123.4, 70.7, 9.74, 3.36.

Cyclopropylmethyl 3,5-dinitrobenzoate 8d. Crystallised from ether (mp 103–105 °C). ^{1}H NMR δ ($X\Delta X\lambda_3$) 0.42 (2H), 0.69 (m, 2H), 1.32 (m, 1H), 4.28 (d, J = 7.6), 9.19 (d, J = 1.9, 2H), 9.23 (t, J = 1.9, 1H); ^{13}C NMR δ ($CDCl_3$) 162.6, 148.6, 134.2, 129.5, 122.2, 71.9, 9.7, 3.6.

Cyclopropylmethyl 2,4-dinitrobenzenesulfenate 8c. Crystallised from methanol (mp 90–91 °C). ^{1}H NMR δ ($CDCl_3$) 0.39 (m, 2H), 0.68 (m, 2H), 1.29 (m, 1H), 3.8 (d, J = 7.3, 2H), 8.0 (d, J = 9.1, 1H), 8.5 (dd, J = 2.2, 9.1, 1H), 9.13 (d, J = 2.2, 1H). ^{13}C NMR δ ($CDCl_3$) 154.8, 144.3, 139.2, 127.7, 123.4, 121.1, 82.8, 11.2, 3.8.

Cyclopropylmethyl 2,4-dinitrobenzoate 8b. Crystallised from pentane (mp 49–51 °C). ^{1}H NMR 300 MHz δ 0.32 (m, 2H), 0.67 (m, 2H), 1.35 (m, 1H), 4.16 (d, J = 7.3, 1H), 7.86 (d, J = 8.3, 1H), 8.52 (dd, J = 8.4, 2.2 Hz, 1H), 8.78 (d, J = 2.2, 1H). ^{13}C NMR δ ($CDCl_3$) 163.7, 148.8, 133.0, 131.2, 127.4, 119.4, 72.2, 9.3, 3.3.

Dicyclopropylmethyl *p*-nitrobenzoate 9d. Crystallised from pentane (mp 65–68 °C). ^{1}H NMR δ ($CDCl_3$) 0.39 (m, 4H), 0.56 (m, 4H), 1.17 (m, 2H), 4.19 (t, J = 6.8Hz) 8.24 (d, J = 7.4, 2H), 8.29 (d, J = 7.4); ^{13}C NMR, δ ($CDCl_3$) 164.4, 150.3, 136.3, 130.7, 123.4, 84.0, 14.7, 2.8, 2.95.

Dicyclopropylmethyl 2,4-dinitrobenzenesulfenate 9b. Crystallised from CH_2Cl_2 (mp 113–116 °C). ^{1}H NMR δ ($CDCl_3$) 0.50 (m, 4H), 0.66 (m, 4H), 1.22 (m, 2H), 4.08 (t, J = 8.6), 7.9 (d, J = 10 Hz, 1H), 8.5 (1H, dd, J = 2.2, 10 Hz), 8.8 (d, J = 2.2 Hz).

X-ray crystallography

Intensity data were collected with a Bruker SMART Apex CCD detector using MoKα radiation (graphite crystal monochromator λ = 0.71073). The temperature was maintained at 130.0(1) using an Oxford Cryostream cooling device. Data were reduced using the program SAINT.[24] The structure was solved by direct methods and difference fourier synthesis using the SHELX[25] suite of programs as implemented with the WINGX[26] software.†

References

1 J. M. White and C. I. Clark, *Topics in Stereochemistry*, ed. S. E. Denmark, John Wiley and Sons, New York, 1999, vol. 22, ch. 3, p. 137.
2 P. Deslongchamps, Stereoelectronic Effects in Organic Chemistry, *Organic Chemistry Series Volume 1*, ed. J. E. Baldwin, Pergamon Press, Oxford, 1983.
3 (*a*) R. S. Mulliken, *J. Chem. Phys.*, 1939, **7**, 339; (*b*) A. N. Egorochkin, *Russ. Chem. Rev.*, 1984, **53**, 445; (*c*) R. Gleiter, *Pure Appl. Chem.*, 1987, **59**, 1585; (*d*) N. Muller and R. S. Mulliken, *J. Am. Chem. Soc.*, 1958, **80**, 3489.
4 D. D. Davis, *J. Organomet. Chem.*, 1981, **206**, 21; M. A. Cook, C. Eaborn and D. R. M. Walton, *J. Organomet. Chem.*, 1970, **24**, 293.
5 W. Hanstein, H. J. Berwin, T. G. Traylor and T. G., *J. Am. Chem. Soc.*, 1970, **92**, 829.
6 W. Adcock, D. P. Cox and W. Kitching, *J. Organomet. Chem.*, 1977, **133**, 393.
7 I. V. Alabugin, *J. Org. Chem.*, 2000, **65**, 3910.
8 A. J. Briggs, R. Glenn, P. G. Jones, A. J. Kirby and P. Ramaswamy, *J. Am. Chem. Soc.*, 1984, **106**, 6200.
9 R. D. Amos, N. C. Handy, P. G. Jones, A. J. Kirby, J. K. Parker, J. M. Percy and M. D. Su, *J. Chem. Soc., Perkin Trans. 2*, 1992, **4**, 549.
10 A. J. Green, J. Giordano and J. M. White, *Aust. J. Chem.*, 2000, **53**, 285.
11 M. Spiniello and J. M. White, *Org. Biomol. Chem.*, 2003, **1**, 3094.
12 (*a*) A. J. Kirby, *The Anomeric Effect and Related Stereoelectronic Effects at Oxygen*, ed. K. Hafner, J.-M. Lehn, C. W. Rees, P. van Rague Schleyer, B. M. Trost and R. Zahradnik, Springer-Verlag, Berlin, 1983.
13 J. B. Lambert, *Tetrahedron*, 1990, **46**, 2677.
14 R. Gleiter, G. Jahne, M. Oda and M. Iyoda, *J. Org. Chem.*, 1985, **50**, 678.
15 E. Uggerud, D. Arad, Y. Apeloig and H. Schwarz, *J. Chem. Soc., Chem. Commun.*, 1989, 1015.
16 T. G. Traylor, W. Hanstein, H. J. Berwin, N. A. Clinton and R. S. Brown, *J. Am. Chem. Soc.*, 1971, **93**, 5715.
17 A. Streitwieser Jr. and S. Alexandratos, *J. Am. Chem. Soc.*, 1978, **100**, 1979.
18 A. de Meijere, *Angew. Chem., Int. Ed. Engl.*, 1979, **18**, 809.
19 H. C. Brown and E. N. Peters, *J. Am. Chem. Soc.*, 1973, **95**, 2400.
20 Y. Apeloig and D. Arad, *J. Am. Chem. Soc.*, 1985, **107**, 5285.
21 F. H. Allen, O. Kennard, R. Taylor and R., *Acc. Chem. Res.*, 1983, **16**, 146.
22 H. Hart and O. E. Curtis Jr., *J. Am. Chem. Soc.*, 1956, **78**, 112.
23 W. D. Clossen and G. T. Kwiatowski, *Tetrahedron*, 1965, **21**, 2779.
24 *Siemens 1999, SMART, SAINT, SADABS*, Siemens Analytical X-ray Instruments Inc., Madison, Wisconsin, USA.
25 *SHELX97 [includes SHELXS97, SHELXL97]–Programs for solution of crystal structures (release 97-2)*, G. M. Sheldrick, Institut fur Anorganische Chemie der Universitat, Tammanstrasse 4, D-3400 Gottingen, Germany, 1998.
26 L. J. Farrugia, *J. Appl. Crystallogr.*, 1999, **32**, 837.

† CCDC reference numbers 265209–265216. See http://www.rsc.org/suppdata/ob/b5/b503124a/ for crystallographic data in CIF or other electronic format.